



**HAL**  
open science

## **NOX4 activity is determined by mRNA levels and reveals a unique pattern of ROS generation**

Lena Serrander, Laetitia Cartier, Karen Bedard, Botond Banfi, Bernard Lardy, Olivier Plastre, Andrzej Sienkiewicz, Laszlo Fórró, Werner Schlegel, Karl-Heinz Krause

### ► To cite this version:

Lena Serrander, Laetitia Cartier, Karen Bedard, Botond Banfi, Bernard Lardy, et al.. NOX4 activity is determined by mRNA levels and reveals a unique pattern of ROS generation. *Biochemical Journal*, 2007, 406 (1), pp.105-114. 10.1042/BJ20061903. hal-00478728

**HAL Id: hal-00478728**

**<https://hal.science/hal-00478728>**

Submitted on 30 Apr 2010

**HAL** is a multi-disciplinary open access archive for the deposit and dissemination of scientific research documents, whether they are published or not. The documents may come from teaching and research institutions in France or abroad, or from public or private research centers.

L'archive ouverte pluridisciplinaire **HAL**, est destinée au dépôt et à la diffusion de documents scientifiques de niveau recherche, publiés ou non, émanant des établissements d'enseignement et de recherche français ou étrangers, des laboratoires publics ou privés.

**NOX4 activity is determined by mRNA levels and reveals a unique pattern  
of ROS generation**

Lena Serrander \*<sup>1</sup>, Laetitia Cartier †, Karen Bedard †, Botond Banfi ‡, Bernard Lardy §,  
Olivier Plastre †, Andrzej Sienkiewicz ||, László Fórró ||, Werner Schlegel \* and Karl-Heinz  
Krause †

\*Phone: +41-22 382 72 33, Fax: +41 22 347 59 79,

E-mail: [Lena.Serrander@medecine.unige.ch](mailto:Lena.Serrander@medecine.unige.ch)

\* Foundation for Medical Research, University of Geneva, 64 av de la Roseraie,  
1205, Geneva, Switzerland

† Department of Immunology and Pathology, University of Geneva,  
Rue Michel Servet 1, 1206 Geneva, Switzerland

‡ Department of Anatomy and Cell Biology, Roy J. and Lucille A. Carver College of  
Medicine, University of Iowa, Iowa City, 52242, USA

§ Department of Enzymology, GREPI, Hôpital Albert Michallon,  
BP 217-CHU Grenoble Cedex 9, France.

|| Institute of Physics of Complex Matter, École Polytechnique Fédérale de Lausanne,  
1015 Lausanne, Switzerland

Short title: Generation of an inducible NOX4-expressing cell line (46)

## Summary

NOX4 is an enigmatic member of the NOX family of ROS-generating NADPH oxidases. NOX4 has a wide tissue distribution, but the physiological function and activation mechanisms are largely unknown, and its pharmacology poorly understood. We have generated cell lines expressing NOX4 upon tetracycline induction. Tetracycline induced a rapid increase in NOX4 mRNA (1 h) followed closely (2h) by a release of reactive oxygen species (ROS). Upon tetracycline withdrawal, NOX4 mRNA levels and ROS release decreased rapidly (<24h). In membrane preparations, NOX4 activity was selective for NADPH over NADH and did not require the addition of cytosol. The pharmacological profile of NOX4 was distinct from other NOX isoforms: diphenyl iodonium (DPI) and thioridazine efficiently inhibited the enzyme, while apocynin and gliotoxin, did not ( $IC_{50} > 100 \mu M$ ). The pattern of NOX4-dependent ROS generation was unique: i) ROS release upon NOX4 induction was spontaneous without need for a stimulus, and ii) the type of ROS released from NOX4 expressing cells was hydrogen peroxide, while superoxide was almost undetectable. Probes that allow detection of intracellular superoxide generation yielded differential results: DHE fluorescence and ACP ESR measurements did not detect any NOX4 signal, while a robust signal was observed with NBT. Thus, most likely NOX4 generates superoxide within an intracellular compartment that is accessible to NBT, but not to DHE and ACP. In conclusion, NOX4 has a distinct pharmacology and pattern of ROS generation. The close correlation between NOX4 mRNA and ROS generation might hint towards a function as inducible NOX isoform.

Key Words: NADPH oxidases, ROS, hydrogen peroxide, superoxide, NOX4, NOX4 inhibitors

Abbreviations:

ROS; reactive oxygen species,

NOX; NADPH oxidases,

HEK cells; human embryonic kidney cells,

TC; tetracycline,

T-REx HEK; tet-operon repressor expressing HEK,

DPI; diphenyleneiodonium chloride

ACP; 1-Acetoxy-3-carboxy-2,2,5,5-tetramethylpyrrolidine

DHE; Dihydroethidium

NBT; nitro blue tetrazolium

Cyt. C; cytochrome C

PKC; protein kinase C

## INTRODUCTION

NOX4 is a member of the NOX family of NADPH oxidases. These enzymes transport electrons from cytoplasmic NADPH across cell and organelle membranes to generate superoxide and down-stream reactive oxygen species (ROS). NOX enzymes have been shown to be involved in the regulation of a wide range of physiological functions, including cell death and survival, differentiation, proliferation,  $\text{Ca}^{2+}$  signalling, gene expression, and migration (reviewed in [1, 2]).

NOX4 was first described in 2000 [3, 4]. The enzyme is highly expressed in kidney, particularly in the tubular system [3]. However NOX4 is also expressed in many other cell types including endothelial cells [5], osteoclasts [6], smooth muscle cells [7], fibroblasts [8], mesangial cells [9], adipocytes [10], pancreatic islets [11] and embryonic stem cells [12]. It has been suggested to be involved in stress signals in kidney [9, 13] and smooth muscle cells [14], TGF $\beta$ -induced differentiation [8, 15, 16], insulin signaling [10], oxygen sensing [17, 18], cardiac differentiation [12], and transcriptional regulation [19, 20].

NOX4 expression is increased by TGF $\beta$  stimulation in fibroblasts [8, 15] as well as by angiotensin stimulation of mesangial cells in the kidney [9]. These stimulations were paralleled with an increase in ROS generation suggesting that NOX4 activity is regulated, at least in part, at the transcriptional level.

While NOX1, NOX2, and NOX3 activity depends on the presence of activator or organizer subunits (NOXAs and NOXOs) [2], NOX4 is active in cells that do not express such cytoplasmic subunits. NOX4 does require the membrane-associated subunit p22<sup>phox</sup> for function [21], however, as opposed to NOX1-3, it does not require the organizer subunit-interacting proline-rich domain of p22<sup>phox</sup> [22]. Data concerning its dependence on the small GTPase Rac and on the need for cell stimulation are contradictory. While some indirect data raise the possibility of Rac involvement, reconstitution data in a variety of cell types suggest that NOX4 activity does not require Rac and is constitutive [21, 23, 24].

This constitutive activity of NOX4 upon heterologous expression is an interesting, but experimentally challenging feature. It raises the possibility that NOX4 might be an inducible NOX isoform, regulated on the level of mRNA level, rather than through post-translational protein modifications. However, this feature also presents a challenge for the study of NOX4 due to the toxicity associated with sustained ROS generation, as evidenced by cellular senescence upon heterologous NOX4 expression [3, 4].

In this study we report the generation of a cell line that expresses NOX4 upon tetracycline-induction. We use this system to study basic features of NOX4 activity and its unusual pattern of ROS generation.

## **EXPERIMENTAL**

### **Material**

Dulbecco's modified Eagle Medium (DMEM), Hank's buffered salt solution, Gateway cloning system including pENTRY and DEST 30 vectors, superscript II, fetal calf serum, blasticidin, neomycin (G418, geneticin), tetracycline (TC), cloning primers, calcein, and amplex red were purchased from Invitrogen. RNeasy columns and DNase were purchased from Qiagen. Scopoletin, horse radish peroxidase (HRP), luminol, cytochrome C, diphenylene iodonium chloride (DPI), thioridazine and apocynin were purchased from Sigma Aldrich. Human kidney RNA was purchased from Clontech.

### **Cloning of human NOX4**

Reverse transcription was carried out on human kidney RNA with superscript II (Invitrogen) according to the manufacturer's instructions. The full-length human NOX4 was amplified by PCR using the following primers:

NOX4\_F: GGGGACAAGTTTGTACAAAAAAGCAGGCTTCACCATG  
GCTGTGTCCTGGAGG

NOX4\_R:

GGGGACCACTTTGTACAAGAAAGCTGGGTCTCAGCTGAAAGACTCTTTATTGTAT  
TC

The PCR product was cloned into a p221 vector (Invitrogen) and transferred into a pDEST 30 vector carrying a tet-on CMV promoter using the Invitrogen Gateway cloning system, according to the manufacturer's instructions.

### **Generation of inducible and stable cell lines**

HEK293 cells over-expressing a tetracycline receptor (T-REx HEK, Invitrogen) were transfected with the NOX4-containing tet-on vector (NOX4-pDEST30) by the calcium phosphate method [25], and selected with 400 µg/ml neomycin (G418) starting 3 days after transfection. HEK293 cells stably expressing NOX4 and NOX5 respectively were obtained by transfection of pcDNA3.1 with the full-length murine NOX4 or full-length human NOX5β

cDNA inserted with neomycin as resistance gene followed by clone selection after neomycin culture for 10-14 days [23].

### Cell culture

All cells were cultured in DMEM (cat no 61965, Invitrogen), 4.5 g/l glucose, supplemented with 10% foetal calf serum and penicillin (100 u/ml) and streptomycin 100 µg/ml at 37°C in air with 5% CO<sub>2</sub>. Selecting antibiotics, blasticidin (5 µg/ml) and neomycin (400 µg/ml), were maintained in transfected cell cultures throughout.

### ROS measurements

#### *Scopoletin, Amplex Red, Cytochrome C reduction and luminol*

Extracellular hydrogen peroxide was measured by either Scopoletin or *Amplex Red*. Scopoletin measurements were performed as previously described scopoletin [26], with minor modifications. Briefly, detached cells (20 000) were plated in 0.2 mL volume of HBSS containing 20 µM scopoletin and 0.5 U/ml horseradish peroxidase, and where indicated, stimuli and/or inhibitors. The plate was kept at 37°C and fluorescence readings were taken every minute for 40-60 minutes with excitation and emission wavelengths of 350 nm and 460 nm respectively in a Victor3 Wallac or BMG Fluostar microplate reader.

Amplex Red measurements were done according to manufacturers instructions, with minor modifications. Briefly, detached cells (50 000) were plated in 0.2 mL volume of HBSS containing 20 µM Amplex Red and 0.1 U/ml horseradish peroxidase, and where indicated, stimuli and/or inhibitors. The plate was kept at 37°C and fluorescence readings were taken every minute for 40-60 minutes with excitation and emission wavelengths of 550 nm and 600 nm respectively in a BMG Fluostar microplate reader.

Extracellular superoxide was measured by either *Cytochrome C* reduction or luminol, as described previously, with minor modifications [23]. For *Cytochrome C*, detached cells (20 000) were plated in 0.2 mL volume of HBSS containing 150 µM *Cytochrome C*, and where indicated, stimuli and/or inhibitors. The plate was kept at 37°C and readings of the absorbance at 550 nm were taken every minute for 40-60 minutes in a Victor3 Wallac or BMG Fluostar microplate reader.

For luminol, detached cells (20 000) were plated in 0.2 mL volume of HBSS containing

10  $\mu\text{M}$  luminol, 0.5 U/ml HRP, and where indicated, stimuli and/or inhibitors. The plate was kept at 37°C and light emission was recorded continuously using a Victor3 Wallac or a BMG Fluostar microplate reader.

*Dihydroethidium (DHE)*: Cells were plated in 96 well plates and in the case of NOX4, induced with TC, 24 prior to experiments. DHE (5  $\mu\text{M}$ ) was added to each well 5 min before addition of stimuli. Fluorescence (490nm/600nm, ex/em) was recorded during 60 min, once per minute in a Fluostar microplate reader at 37°C.

*Nitro blue tetrazolium (NBT)*: Cells were plated in 12 well plates and in the case of T-REx NOX4, induced with TC, 24 prior to experiments. Cells were washed in HBSS and incubated with NBT (1.6 mg/ml) in HBSS at 37°C for 45 min. After fixation in 100% methanol and a wash in methanol, the formazan precipitates were dissolved by addition of 560  $\mu\text{l}$  2M KOH and 480  $\mu\text{l}$  DMSO. The amount of reduced NBT was quantified by determination of OD at 630 nm. Photographs were taken before fixation, using a Nikon Coolpix CCD camera (Nikon) mounted on an Axiovert S100 microscope (Zeiss) using a 100X objective.

*Electron spin resonance (ESR)*: Cells were detached and resuspended in HBSS (supplemented with  $\text{Ca}^{2+}$  and  $\text{Mg}^{2+}$ ) to  $1 \times 10^7/\text{ml}$  and incubated with 100  $\mu\text{M}$  ACP for 45 min at 37°C. For performing ESR measurements, aliquots of approximately 12  $\mu\text{l}$  were transferred into 1.0 mm ID /1.2 mm OD quartz capillary tubes from VitroCom, NJ, USA (sample height of 50 mm) and sealed on both ends with Cha-Seal<sup>TM</sup> tube sealing compound (Medex International, Inc., USA). ESR experiments were carried out at room temperature using an ESP300E spectrometer (Bruker BioSpin GmbH, Karlsruhe, Germany), which was equipped with a standard rectangular mode TE<sub>102</sub> cavity. Instrument settings were: microwave power 20mW, microwave frequency 9.775 GHz, magnetic field 3480 $\pm$ 60 G, modulation frequency 100 kHz, modulation amplitude 1.045 G, receiver gain  $2 \times 10^3$ , time constant 20.48 ms, conversion time 40.96 ms, and total scan time 41.9 s. Five-scan field-swept spectra were accumulated for each ESR trace.

### **Quantification of cell numbers**

Cell numbers were determined by calcein fluorescence in order to calculate the amount of hydrogen peroxide produced/cells using 490 nm excitation and 520 nm emission filters in separate wells after 10 min incubation with calcein (2.5  $\mu\text{M}$ ) at 37°C and normalized to a standard curve of counted cell numbers.



### **ROS measurements in membranes preparations**

Membrane were prepared as described previously [27]. Protein concentration was determined with Bradford reagent using bovine serum albumin as a standard. ROS activity was determined with the amplex red method described above with 5 µg protein/96-well containing 25 µM amplex red and 0.1 U/ml HRP in HBSS (with Ca<sup>2+</sup> and Mg<sup>2+</sup>).

### **Real time PCR**

Total RNA was isolated according to manufacturer's instructions using RNeasy (Qiagen). cDNA was synthesized from 0.5 µg RNA, using a mix of oligo-dT and random hexamers, with Superscript II reverse transcriptase (Invitrogen) according to manufacturer's instructions. The cDNA equivalent to 5 ng of total RNA was robot-pipetted and PCR-amplified in a final volume of 10 µl in triplicates in an ABI PRISM 7700 detection system (PE-Applied Biosystems).

Primers for the reference genes TATA-box-binding protein (TBP), β-glucuronidase (GusB) and Elongation factor-1 alpha 1 (EEF1A1) (see probe and primer sequences in table I), were designed by Primer Express 2.0 (Applied Biosystems, Foster City, CA). NOX4 was detected with primers and probe from Assay-on-Demand® no Hs00276431 from Applied Biosystems. The quantitative PCR experiments and analysis were done with the help of the Genomic platform, Geneva.

### **Statistics**

Results are expressed as mean ± standard error of the mean (SEM) of 3-8 experiments performed independently. Paired Student's t-test or ANOVA were performed when indicated and p<0.05 were considered significant and marked \* for p<0.01 with \*\* and p<0.001 with \*\*\*.

## **RESULTS**

### **ROS generation in a tetracycline-inducible NOX4 system**

Because NOX4 is constitutively active upon heterologous expression, we generated a tetracycline inducible system that allowed controlled NOX4 expression. We used the T-REx system which is based on the expression of a tet repressor that binds to a modified CMV promoter and thereby maintains the latter in an inactive state. Tetracycline binds to the tet

repressor removing it from the promoter and thereby permitting transcription. As the tet-repressor expressing HEK293 cells (T-REx cells) were established with a blasticidin resistance, blasticidin was continuously included in the culture medium to ensure high level expression of the tet repressor, which is important to minimize residual expression (leaking).

To generate inducible NOX4 cells, the T-REx cells were transfected with a vector construct carrying the full-length human NOX4 cDNA driven by the modified CMV promoter. After 14 days of neomycin selection, several clones were established and investigated for the release of ROS upon tetracycline-induction using a scopoletin assay. Among 6 clones tested, the increase in the rate of ROS production upon TC induction ranged from no change to 161 times that of un-induced cells (data not shown). Fig. 1a shows the clone selected for further experiments. In the absence of tetracycline, there is no detectable release of ROS into the medium. Tetracycline did not lead to ROS release in non-transfected cells (i.e. cells expressing the tet repressor only), nor did it enhance ROS release in cells stably expressing NOX4 (Fig. 1b).

Quantitative analysis of ROS release using the amplex red technique yielded the following results: non-transfected HEK T-REx cells generated less than 0.2 fmoles  $H_2O_2$ /cell/h. Non-induced NOX4 T-REx HEK cells produced  $1.5 \pm 0.8$  fmoles  $H_2O_2$ /cell/h, while tetracycline-induced cells ( $1 \mu\text{g/ml}$ , 24h) generated  $83 \pm 24$  fmoles  $H_2O_2$ /cell/h after a 24 hour TC induction ( $n=6$ ). To put these numbers into context, tetracycline-induced NOX4 cells released roughly equal amounts of  $H_2O_2$ /cell as a reconstituted NOX2 system in HEK cells (data not shown) or NOX5-expressing HEK cells (see below), but approximately a 5-10 times less than PMA-stimulated neutrophils (data not shown). Thus, the capacity of NOX4 is probably in a similar range to that of other NOX enzymes.

We next investigated the effect of tetracycline concentration in the system. Cells were induced with tetracycline concentrations ranging from  $1.25 \text{ fg/ml}$  to  $10 \mu\text{g/ml}$  and NOX4 activity was assessed by ROS generation (Fig. 2). In the absence of tetracycline, background ROS generation was below 3% of that in cells induced with  $1 \mu\text{g/ml}$  TC. The EC 50 for tetracycline was  $91 \text{ pg/ml}$ . We chose a concentration of  $1 \mu\text{g/ml}$  for further experiments since this concentration was well within the plateau range without apparent toxic effects.

### **Time course of induction of mRNA and functional activity**

We investigated the time course of NOX4 induction by tetracycline. Both, NOX4 mRNA and ROS production showed a time-dependent increase (Fig 3a and b). However mRNA

elevations were detected earlier than the increased ROS generation (1 and 2 hours after tetracycline addition, respectively). The fact that ROS generation was detectable after 2 hours suggests a relatively rapid transcriptional and translational processing of NOX4. Longer times of tetracycline induction resulted in a slight reduction of activity possibly reflecting cell toxicity (data not shown).

In order to investigate the reversibility of the NOX4 induction, we followed NOX4 mRNA levels and ROS generation after tetracycline withdrawal. NOX4 mRNA levels decreased by more than 50% after 4 hours, while a 50% decrease in ROS required more than 8 hours (Fig 3 c and d).

### **NOX4 activity in membrane fractions: independence of cytosol and selectivity for NADPH over NADH**

We next investigated ROS generation in membrane fractions without added cytosol using amplex red. As shown in Figure 4, a strong signal was only observed with NADPH as electron donor. The signal with NADH was only slightly above background values, demonstrating that NOX4 preferentially uses NADPH. Thus NOX4 is similar to other members of the NOX family, a true NADPH oxidase. No enhancement of activity was obtained by addition of cytosol (data not shown), confirming that NOX4 activity is independent on cytosolic subunits for function. Thus we conclude that NOX4 is, similar to other members of the NOX family, selective for NADPH over NADH.

### **Pharmacological profile of NOX4 activity**

In order to characterize potential inhibitors, four known NOX2 inhibitors were tested for an effect on NOX4 activity (Fig 5). DPI, the most commonly used agent to block NOX activity, and thioridazine, an anti-psychotic drug that inhibits NOX2 activity in neutrophils [28], inhibited NOX4 with high to intermediate affinity, in a concentration range similar to that observed for NOX2. DPI blocked NOX4 activity at concentrations in the submicromolar range (IC<sub>50</sub> of 0.2  $\mu$ M), while thioridazine blocked at low micromolar concentrations (4  $\mu$ M).

In contrast, two other NOX2 inhibitors, which inhibit NOX2 in the low micromolar range inhibited NOX4 only with a very low affinity. Apocynin, which inhibits neutrophil ROS generation with an IC<sub>50</sub> of approximately 10  $\mu$ M [29], had an IC<sub>50</sub> of >200  $\mu$ M for NOX4. Gliotoxin, an aspergillus fumigatus toxin inhibits NOX2 with an IC<sub>50</sub> of 5-10  $\mu$ M [30, 31]. The effect of gliotoxin on NOX4 showed some low efficacy inhibition, but the

maximal inhibition achieved was around 40% with 100  $\mu$ M gliotoxin therefore IC<sub>50</sub> values could not be calculated. Thus, NOX4 has a distinct profile of inhibition as compared to NOX2 (table II).

### **Characteristics of NOX4-dependent ROS generation**

When different techniques to measure ROS release from cells were applied, we found an unusual pattern in NOX4-expressing cells. NOX4 activity induced a strong signal with probes that detect extracellular hydrogen peroxide, such as scopoletin (Fig. 1-2) and amplex red (Fig. 3, 6a and b), but not with probes that detect extracellular superoxide, such as cytochrome C reduction (Fig. 6c,d) and horseradish peroxidase-dependent luminol-enhanced chemiluminescence (Fig. 6e,f). This contrasts with the behaviour of other NOX enzymes, such as NOX5, which yields a strong signal with probes detecting superoxide (Fig 6, c-f). Note that in these studies, PMA-stimulated NOX5 activation was used; the PMA effects on NOX5-expressing cells have characteristics comparable to the previously described ionomycin effects (data not shown and [32]). Note also that NOX4 activity is independent of or even slightly inhibited by PMA (Fig 6b).

Our results suggest that NOX4 either directly generates hydrogen peroxide or that it generates intracellular superoxide which dismutates intracellularly to the membrane permeant hydrogen peroxide. To distinguish between these possibilities, we used techniques to detect intracellular superoxide. The dihydroethidium (DHE)-method has been widely used to detect intracellular superoxide generation. Indeed, the non-fluorescent, membrane-permeant DHE enters cells freely. Upon interaction with superoxide, the membrane impermeant ethidium cation is liberated, which becomes fluorescent upon intercalation DNA. As shown in Fig. 7, no NOX4 signal was detected with the DHE method, while there was a clear NOX5 signal. These results are interesting, but they do not globally exclude an intracellular superoxide generation by NOX4. Indeed a recent study demonstrated that the DHE method does not allow detection of superoxide generated by NOX2 in the phagosome [33].

We next investigated NOX4-dependent ROS generation using electron spin resonance (ESR). With appropriate spin trap agents, ESR can specifically detect superoxide. ACP (1-Acetoxy-3-carboxy-2,2,5,5-tetramethylpyrrolidine) is an ESR spin trap agent that has been shown to enter cells in its ester form which is then hydrolyzed by cytosolic esterases. This hydrolyzed form is able to interact with intracellular superoxide [34, 35]. Thus, ACP is thought to be an appropriate spin trap agent to measure intracellular superoxide generation. NOX4-activity did not lead to a detectable ESR signal, whereas significant signals could be

detected in PMA-stimulated NOX5 cells (Fig 8). However, the design of ACP (i.e. hydrolysis by cytosolic esterases) makes it suited to detect of cytoplasmic superoxide generation, and not for measuring superoxide generation within intracellular organelles.

Thus, the DHE and the ESR results reasonably exclude NOX4-dependent superoxide generation in the cytosol, and probably also in the nucleus and inner mitochondrial space, but they do not exclude the possibility that NOX4-dependent superoxide generation takes place within some other intracellular organelle.

One of the oldest and most established methods to detect intracellular superoxide generation is the reduction of nitro blue tetrazolium (NBT) to formazan, a dark blue precipitate. As NBT needs to be reduced, only superoxide (which may act as electron donor or acceptor), but not hydrogen peroxide (which is exclusively an oxidizing agent) is capable of reacting with NBT. Furthermore, NBT preferentially detects intracellular superoxide [36]. As assessed by a quantitative NBT test (Fig. 9), tetracycline-induced NOX4 cells elicited a significant NBT reduction, as compared to non-induced cells. This signal was completely blocked by DPI (5 $\mu$ M). The NOX4-dependent NBT signal is a good argument in favor of superoxide generation. We can however not formally exclude a diaphorase activity (i.e. NBT would receive electrons directly from NOX4 without a superoxide intermediate). We also analyzed the subcellular distribution of formazan precipitates by light microscopy. No formazan precipitates were observed in uninduced cells (Fig. 9a). In tetracycline-induced cells (Fig. 9b), the precipitates showed a punctuate staining within the cytoplasm. In many cells, this staining was in the perinuclear region, but occasionally also in the cell periphery. The nucleus was systematically spared, but the nuclear envelope (which is part of the endoplasmic reticulum) showed a strong staining.

## Discussion

In this study, an inducible cell line was used to analyze basic biochemical properties of the NOX family NADPH oxidase NOX4. Given the fact that NOX4 generates substantial amounts of ROS without a need for cell stimulation [3, 4, 21], a stable expression system has inherent dangers: i) damage to DNA which could lead to cellular senescence [3] or - in cells with deficient p53 function (e.g. HEK293 cells) - to an accumulation of DNA mutations; ii) damage to mitochondria which may lead to an increased mitochondrial ROS generation; and iii) permanent upregulation of antioxidant responsive genes, which would make it difficult to distinguish the acute NOX4 effects from a long-term antioxidant response. Thus,

an inducible NOX4 system, as described in this manuscript, is preferable to cells stably expressing NOX4.

An additional advantage of the inducible system is that it offers the possibility to study the temporal relationship between mRNA levels and enzyme function. And one of the striking results of our study is that NOX4 mRNA levels are closely followed by NOX4 activity. Unfortunately, there are presently no antibodies reliably recognizing human NOX4. Thus, it is presently not possible to calculate protein half-life. However, our results based on NOX4 function suggest that the NOX4 protein is rapidly (i.e. within a time frame of hours) synthesized and degraded. Note that this is in stark contrast to available data on NOX2, where the protein and its function persist for several days after transcriptional activity is shut down [37]. Obviously, a heterologous expression system cannot determine whether NOX4 is regulated on a transcriptional level [8, 15] in endogenously NOX4 expressing cells. However our results clearly demonstrate that NOX4 has the potential to function as an inducible "iNOX".

To our knowledge, this is the first study of NOX4 activity in a broken cell system. It unequivocally demonstrates that NOX4 is functional in the absence of cytosol, reinforcing the concept that NOX4 activity is independent of cytosolic subunits. Importantly, this system also allowed the study of the NOX4 electron source. It is now clear that NOX2, NOX5, and NOX1 specifically use NADPH, and not NADH, as electron donor (reviewed in [2]). However, it has been suggested that ROS-generating enzymes, in the vascular system, might prefer NADH over NADPH [38] and for that reason several authors still use the term "NAD(P)H oxidase". Our study reveals that NOX4 is indeed an NADPH oxidase with a preference for NADPH over NADH. Thus, we suggest that the term NAD(P)H oxidase should no longer be used when referring to NOX enzymes.

The inhibitor analysis shown in this study is, to our understanding, a first pharmacological profiling of NOX4. Not unexpectedly DPI, a large spectrum inhibitor of electron transporters including various NOX enzymes, mitochondrial oxidase, and xanthine oxidase (reviewed in [2]) was found to inhibit NOX4. The following arguments suggest that the DPI effect is not due mitochondrial inhibition: i) inhibition of ROS generation occurred in the submicromolar range, while inhibition of mitochondrial oxidase occurs with an IC<sub>50</sub> of approximately 10  $\mu$ M DPI [39, 40]; ii) no ROS generation was detected unless NOX4 expression was induced by tetracycline. Thioridazine, another efficient NOX4 inhibitor, lacks specificity, as it also inhibits mitochondrial oxidase and xanthine oxidase in an almost identical concentration range [41, 42]. In contrast, neither apocynin nor gliotoxin are efficient

NOX4 inhibitors. In the case of apocynin, this is expected as apocynin is thought i) to inhibit NOX2 subunit assembly and ii) to require myeloperoxidase-dependent metabolism for full activity [43]. The mode of action of gliotoxin is poorly understood, but clearly it is not a useful NOX4 inhibitor. In conclusion, NOX4 displays a unique pharmacological profile, distinct from that of NOX2 (table II).

The atypical pattern of NOX4-dependent ROS generation identified in this study is most compatible with a NOX4-dependent superoxide generation within a tight intracellular compartment, devoid of DNA. The alternative explanation, namely a direct hydrogen peroxide generation by NOX4 appears less likely since: i) NOX enzymes are mono-electron transporters that transport single electrons across a membrane (reviewed in [2]) ii) hydrogen peroxide does not reduce NBT and there could not account for the observed NBT signal. This conclusion is also in line with a recent study analysing ROS generation in smooth muscle cell membranes [44]. Localization studies of NOX4 are notoriously difficult. Antibody studies suggest a localization close to focal adhesions, within the nucleus or in the endoplasmic reticulum [20, 21, 24]. However, the specificity of currently available NOX4 antibodies is not undisputed. The use of tagged NOX4 is also not without pitfalls, as it is hard to exclude the possibility that the tag alters cellular localization. In addition, C-terminal tags impair NOX4 activity (unpublished data and [21]). With this limitation in mind, N-terminally eGFP-tagged NOX4 yielded interesting results: fluorescence displayed a punctate pattern consistent with intracellular membranes, possibly the endoplasmic reticulum [21, 45]. Our data also support the hypothesis that NOX4 is localized in intracellular membranes. The subcellular localization of NBT precipitation is thought to reflect at least to some extent the site of superoxide generation as the reduced NBT is water-insoluble and precipitates rapidly [36]. Thus, the punctate localization of the formazan precipitations, in particular around the nuclear envelope (Fig.8) is consistent with previous studies which report NOX4 localization in the ER. An ER localization is consistent with the DHE findings. While DHE can freely cross cell membranes, the ethidium cation generated after reduction by superoxide is impermeant. Thus failure of DHE to detect a signal suggests that superoxide is generated within subcellular compartment devoid of nucleic acids, such as the ER.

Fundamentally, there are at least two possible theories to explain the physiological need for a superoxide-producing enzyme within intracellular membranes. NOX4 might regulate the redox environment within an intracellular organelle; this would be particularly pertinent for the endoplasmic reticulum which is supposed to maintain an oxidizing environment in order to assure proper posttranslational processing of proteins. NOX4 might

however also regulate protein oxidation in the region surrounding the organelle through diffusion of hydrogen peroxide. In this case, NOX4 might generate signals including regulation of activity of kinases, phosphatases and transcription factors.

### **Acknowledgements**

We would like to thank the collaborators from the genomics platform of the NCCR, Geneva for assistance with the design of the quantitative PCR experiments, Bianca Mottironi for helpful discussions and Marie-Claude Jaquot for technical assistance. We thank Katarzyna Pierzchała for kind assistance in performing ESR measurements. Vincent Jaquet and Sten Theander are acknowledged for their careful reading of the manuscript. This work was supported by grants from the Swiss National Science Foundations: MHV grant (LS) and project grant 3100A0-103725 (KHK).



References

1. Lambeth, J.D., *NOX enzymes and the biology of reactive oxygen*. Nat Rev Immunol, 2004. **4**(3): p. 181-9.
2. Bedard, K. and K.H. Krause, *The NOX family of ROS-generating NADPH oxidases: physiology and pathophysiology*. Physiol Rev, 2007. **87**: p. 245-313.
3. Geiszt, M., et al., *Identification of renox, an NAD(P)H oxidase in kidney*. Proceedings of the National Academy of Science USA, 2000. **97**(14): p. 8010-8014.
4. Shiose, A., et al., *A novel superoxide-producing NAD(P)H oxidase in kidney*. J Biol Chem, 2001. **276**(2): p. 1417-23.
5. Ago, T., et al., *Nox4 as the major catalytic component of an endothelial NAD(P)H oxidase*. Circulation, 2004. **109**(2): p. 227-33.
6. Yang, S., et al., *A New Superoxide-generating Oxidase in Murine Osteoclasts*. Journal of Biological Chemistry, 2001. **276**(8): p. 5452-8.
7. Ellmark, S.H., et al., *The contribution of Nox4 to NADPH oxidase activity in mouse vascular smooth muscle*. Cardiovasc Res, 2005. **65**(2): p. 495-504.
8. Cucoranu, I., et al., *NAD(P)H Oxidase 4 Mediates Transforming Growth Factor- $\beta$ 1-Induced Differentiation of Cardiac Fibroblasts Into Myofibroblasts*. Circ Res, 2005.
9. Gorin, Y., et al., *Nox4 mediates angiotensin II-induced activation of Akt/protein kinase B in mesangial cells*. Am J Physiol Renal Physiol, 2003. **285**(2): p. F219-29.
10. Mahadev, K., et al., *The NAD(P)H oxidase homolog Nox4 modulates insulin-stimulated generation of H<sub>2</sub>O<sub>2</sub> and plays an integral role in insulin signal transduction*. Mol Cell Biol, 2004. **24**(5): p. 1844-54.
11. Uchizono, Y., et al., *Expression of isoforms of NADPH oxidase components in rat pancreatic islets*. Life Sci, 2006. **80**(2): p. 133-9.
12. Li, J., et al., *The NADPH oxidase NOX4 drives cardiac differentiation: Role in regulating cardiac transcription factors and MAP kinase activation*. Mol Biol Cell, 2006. **17**(9): p. 3978-88.
13. Gorin, Y., et al., *Nox4 NAD(P)H oxidase mediates hypertrophy and fibronectin expression in the diabetic kidney*. J Biol Chem, 2005.
14. Pedruzzi, E., et al., *NAD(P)H oxidase Nox-4 mediates 7-ketocholesterol-induced endoplasmic reticulum stress and apoptosis in human aortic smooth muscle cells*. Mol Cell Biol, 2004. **24**(24): p. 10703-17.
15. Sturrock, A., et al., *Transforming Growth Factor  $\beta$ 1 Induces Nox 4 NAD(P)H Oxidase and Reactive Oxygen Species-Dependent Proliferation in Human Pulmonary Artery Smooth Muscle Cells*. Am J Physiol Lung Cell Mol Physiol, 2005.
16. Hu, T., et al., *Reactive oxygen species production via NADPH oxidase mediates TGF- $\beta$ -induced cytoskeletal alterations in endothelial cells*. Am J Physiol Renal Physiol, 2005. **289**(4): p. F816-25.
17. Maranchie, J.K. and Y. Zhan, *Nox4 is critical for hypoxia-inducible factor 2- $\alpha$  transcriptional activity in von Hippel-Lindau-deficient renal cell carcinoma*. Cancer Res, 2005. **65**(20): p. 9190-3.
18. Lee, Y.M., et al., *NOX4 as an oxygen sensor to regulate TASK-1 activity*. Cell Signal, 2005.
19. Brar, S.S., et al., *An NAD(P)H oxidase regulates growth and transcription in melanoma cells*. Am J Physiol Cell Physiol, 2002. **282**(6): p. C1212-24.
20. Kuroda, J., et al., *The superoxide-producing NAD(P)H oxidase Nox4 in the nucleus of human vascular endothelial cells*. Genes Cells, 2005. **10**(12): p. 1139-51.

21. Martyn, K.D., et al., *Functional analysis of Nox4 reveals unique characteristics compared to other NADPH oxidases*. Cell Signal, 2005. **28**: p. 28.
22. Kawahara, T., et al., *Point mutations in the proline-rich region of p22phox are dominant inhibitors of Nox1- and Nox2-dependent reactive oxygen generation*. J Biol Chem, 2005.
23. Banfi, B., et al., *A Ca(2+)-activated NADPH oxidase in testis, spleen, and lymph nodes*. Journal of Biological Chemistry, 2001. **276**(40): p. 37594-37601.
24. Ambasta, R.K., et al., *Direct interaction of the novel Nox proteins with p22phox is required for the formation of a functionally active NADPH oxidase*. J Biol Chem, 2004. **279**(44): p. 45935-41.
25. Chen, C.A. and H. Okayama, *Calcium phosphate-mediated gene transfer: a highly efficient transfection system for stably transforming cells with plasmid DNA*. Biotechniques, 1988. **6**(7): p. 632-8.
26. De la Harpe, J. and C.F. Nathan, *A semi-automated micro-assay for H<sub>2</sub>O<sub>2</sub> release by human blood monocytes and mouse peritoneal macrophages*. J Immunol Methods, 1985. **78**(2): p. 323-36.
27. Banfi, B., et al., *Mechanism of Ca<sup>2+</sup> activation of the NADPH oxidase 5 (NOX5)*. J Biol Chem, 2004. **279**(18): p. 18583-91.
28. Traykov, T., et al., *Effect of phenothiazines on activated macrophage-induced luminol-dependent chemiluminescence*. Gen Physiol Biophys, 1997. **16**(1): p. 3-14.
29. Van den Worm, E., et al., *Effects of methoxylation of apocynin and analogs on the inhibition of reactive oxygen species production by stimulated human neutrophils*. Eur J Pharmacol, 2001. **433**(2-3): p. 225-30.
30. Tsunawaki, S., et al., *Fungal metabolite gliotoxin inhibits assembly of the human respiratory burst NADPH oxidase*. Infect Immun, 2004. **72**(6): p. 3373-82.
31. Nishida, S., et al., *Fungal metabolite gliotoxin targets flavocytochrome b558 in the activation of the human neutrophil NADPH oxidase*. Infect Immun, 2005. **73**(1): p. 235-44.
32. Jagnandan, D., et al., *Novel Mechanism of Activation of NADPH Oxidase 5: CALCIUM SENSITIZATION VIA PHOSPHORYLATION*. J Biol Chem, 2007. **282**(9): p. 6494-507.
33. Rinaldi, M., et al., *Evaluation of assays for the measurement of bovine neutrophil reactive oxygen species*. Vet Immunol Immunopathol, 2007. **115**(1-2): p. 107-25.
34. Takeshita, K., et al., *In vivo monitoring of hydroxyl radical generation caused by x-ray irradiation of rats using the spin trapping/EPR technique*. Free Radic Biol Med, 2004. **36**(9): p. 1134-43.
35. Yokoyama, H., et al., *In vivo EPR imaging by using an acyl-protected hydroxylamine to analyze intracerebral oxidative stress in rats after epileptic seizures*. Magn Reson Imaging, 2000. **18**(7): p. 875-9.
36. Berridge, M.V., P.M. Herst, and A.S. Tan, *Tetrazolium dyes as tools in cell biology: new insights into their cellular reduction*. Biotechnol Annu Rev, 2005. **11**: p. 127-52.
37. Borregaard, N., *Development of neutrophil granule diversity*. Ann N Y Acad Sci, 1997. **832**: p. 62-8.
38. Griendling, K.K., et al., *Angiotensin II stimulates NADH and NADPH oxidase activity in cultured vascular smooth muscle cells*. Circulation Research, 1994. **74**(6): p. 1141-1148.
39. Hool, L.C., et al., *Role of NAD(P)H oxidase in the regulation of cardiac L-type Ca<sup>2+</sup> channel function during acute hypoxia*. Cardiovasc Res, 2005. **67**(4): p. 624-35.

40. Li, Y. and M.A. Trush, *Diphenyleneiodonium, an NAD(P)H oxidase inhibitor, also potently inhibits mitochondrial reactive oxygen species production*. *Biochem Biophys Res Commun*, 1998. **253**(2): p. 295-9.
41. Rodrigues, T., et al., *Thioridazine interacts with the membrane of mitochondria acquiring antioxidant activity toward apoptosis--potentially implicated mechanisms*. *Br J Pharmacol*, 2002. **136**(1): p. 136-42.
42. Hadjimitova, V., et al., *Effect of some psychotropic drugs on luminol-dependent chemiluminescence induced by O<sub>2</sub><sup>-</sup>, \*OH, HOCl*. *Z Naturforsch [C]*, 2002. **57**(11-12): p. 1066-71.
43. Stolk, J., et al., *Characteristics of the inhibition of NADPH oxidase activation in neutrophils by apocynin, a methoxy-substituted catechol*. *Am J Respir Cell Mol Biol*, 1994. **11**(1): p. 95-102.
44. Clempus, R.E., et al., *Nox4 is required for maintenance of the differentiated vascular smooth muscle cell phenotype*. *Arterioscler Thromb Vasc Biol*, 2007. **27**(1): p. 42-8.
45. Van Buul, J.D., et al., *Expression and localization of NOX2 and NOX4 in primary human endothelial cells*. *Antioxid Redox Signal*, 2005. **7**(3-4): p. 308-17.
46. Hancock, J.T. and O.T. Jones, *The inhibition by diphenyleneiodonium and its analogues of superoxide generation by macrophages*. *Biochem J*, 1987. **242**(1): p. 103-7.
47. Hampton, M.B. and C.C. Winterbourn, *Modification of neutrophil oxidant production with diphenyleneiodonium and its effect on bacterial killing*. *Free Radic Biol Med*, 1995. **18**(4): p. 633-9.
48. Ali, M.H., et al., *Mitochondrial requirement for endothelial responses to cyclic strain: implications for mechanotransduction*. *Am J Physiol Lung Cell Mol Physiol*, 2004. **287**(3): p. L486-96.
49. Kweon, Y.O., et al., *Gliotoxin-mediated apoptosis of activated human hepatic stellate cells*. *J Hepatol*, 2003. **39**(1): p. 38-46.

## Figure legends

### Figure 1

#### ROS release in tetracycline-inducible NOX4 cells

Tet repressor-expressing HEK293 cells (T-REx cells) were transfected with an expression plasmid containing the human NOX4 sequence under the control of a modified CMV promoter as well as a neomycin selection cassette. After neomycin-selection, clones were analysed for ROS release without or with tetracycline (24h) using a scopoletin fluorescence assay (Fig 1a). Figure 1b shows scopoletin measurements in tet repressor-expressing (T-REx) HEK293 cells without NOX4 transfection as well as from stable cell lines expressing NOX4 continuously, with and without tetracycline.

Panels show representative traces; similar results were obtained on at least three independent occasions.

### Figure 2

#### Induction of NOX4 mRNA and ROS release as a function of tetracycline concentration in inducible NOX4 cells

NOX4 T-REx HEK293 cells (clone 20) were incubated for 24 hours with tetracycline (1.25 fg/ml to 10 µg/ml). The ROS release is presented as relative scopoletin fluorescence/h (100 corresponds to cells induced with 1 µg/ml tetracycline). The dose-response curve was fitted with a 4-parameter Hill sigmoid curve for the determination of the EC50 (n=4 independent experiments).

### Figure 3

Close temporal correlation between induction of NOX4 mRNA and activity after TC-induction and omission

T-REx NOX4 HEK cells were induced for NOX4 by addition of 1  $\mu\text{g/ml}$  TC for the times indicated (upper panels). In the lower panels, TC was withdrawn after 24 hours and the run-down was assessed at indicated time-points.

a) NOX4 mRNA was determined by qPCR, normalized to three house-keeping genes and shown here as fold-increase over non-induced NOX4 T-REx cells. b) NOX4 activity was measured as  $\text{H}_2\text{O}_2$  production/hour using amplex red and shown here as fold increase in hydrogen peroxide produced over non-induced cells. (n=4 independent experiments)

c) NOX4 mRNA was determined by qPCR, normalized to three house-keeping genes and shown as percent of NOX4 mRNA after 24 hours TC-induction d) NOX4 activity was measured as  $\text{H}_2\text{O}_2$  production/hour using amplex red and shown here as % of hydrogen peroxide produced by TC-induced cells after 24 hours TC-induction. (n=3-8 independent experiments)

#### Figure 4

NOX4 is an NADPH dependent oxidase

T-REx NOX4 cells were induced with 1  $\mu\text{g/ml}$  TC 24 h, followed by lysis and membrane preparation. Membranes (5  $\mu\text{g/well}$ ; no addition of cytosol) were added to an amplex red mix in a final volume of 200  $\mu\text{l}$ . NADPH and NADH was added and mixes incubated for 20 min at 37°C before ROS production was measured by amplex red fluorescence. Results are shown as end values. (mean  $\pm$  SEM, n=3-4 independent experiments).

### Figure 5

#### Effect of inhibitors on NOX4 activity

T-REx NOX4 cells were induced with 1  $\mu\text{g/ml}$  TC for 24 hours prior to measurements. DPI (a) Apocynin (b), gliotoxin (c) or thioridazine (d) were added at different concentrations and NOX4 activity was measured by amplex red fluorescence. Fluorescence values from 50 000 cells were recorded after 20 min and normalised to those obtained from NOX4-induced cells without inhibitor. A 4-parameter Hill sigmoid curve was used for the determination of IC<sub>50</sub> values. (mean  $\pm$  SEM, n=3 independent experiments)

### Figure 6

Hydrogen peroxide is the major oxidative metabolite measured from NOX4-induced cells. Cells (20 000/well) were added to detection mixes for amplex red (hydrogen peroxide detection), cytochrome C (superoxide detection) and luminol (superoxide detection) respectively. Signals were recorded for 60 min. DPI was used at 5  $\mu\text{M}$  final concentration where indicated. Left panels (a, c, e) show representative traces from each set of experiments and right panels (b, d, f) show the mean and standard error of the mean (SEM) from accumulated signals after 1 hour (amplex red and cytochrome C) and peak signal (luminol) from 3-8 different experiments (mean  $\pm$  SEM).

### Figure 7

Dihydroethidium does not detect a signal from NOX4-expressing cells

DHE (5  $\mu\text{M}$ ) was added to adherent cells and fluorescence measured for 60 min (Fig 9a).

Panel a shows a trace from representative experiment and panel b depicts delta values after 60 min (mean  $\pm$  SEM, n=3-5 independent experiments).

### Figure 8

ESR detects superoxide in NOX5 cell, but not in NOX4 induced cells

Cells were detached and resuspended in HBSS to 10 million/ml, incubated with the spin probe ACP (100  $\mu$ M) for 45 min at 30°C before cell suspension was drawn up in capillaries and placed in the ESR spectrometer. Panel a and b shows a representative ESR traces from NOX5 cells stimulated with PMA and TC-induced NOX4 cell respectively. Fig 8c shows a mean of peak ESR signal for each condition (mean  $\pm$  SEM, n=3 independent experiments).

### Figure 9

Intracellular ROS detection with NBT is positive for NOX4 expressing cells

NBT (1.6 mg/ml) was added and plates incubated at 37°C for 45 minutes.

Micrographs show NBT tests from a) non-induced NOX4 cells and b) TC-induced NOX4 cells respectively. Panel c shows quantification of dissolved formazan by absorbance quantification at 630 nm of from non-induced and TC-induced NOX4 (n=3-5 independent experiments).

Table titles

Table I

Primers for quantitative PCR

Table II

A comparison of the effect on various inhibitors on NOX4 as well as on NOX2 and mitochondrial ROS generation



Table I

<i>primer</i>	<i>Sequence</i>
Hs-TBP_for	GCCCGAAACGCCGAATATA
Hs-TBP_rev	CGTGGCTCTCTTATCCTCATGA
Hs-GusB_for	CCACCAGGGACCATCCAAT
Hs-GusB_rev	AGTCAAAATATGTGTTCTGGACAAAGTAA
Hs-EEF1A1_for	AGCAAAAATGACCCACCAATG
Hs-EEF1A1_rev	GGCCTGGATGGTTCAGGATA
<i>Probe</i>	
Hs-TBP_T	CCGCAGCAAACCGCTTGGGA
Hs-GusB_T	CCTGACTGACACCTCCAAGTATCCCAAGG
Hs-EEF1A1_T	CACCTGAGCAGTGAAGCCAGCTGCTT

Table II

Inhibitor	NOX4 IC50 μM	NOX2 IC50 μM	mitochondrial oxidase IC50 μM
DPI	.2	0.9 [46] 0.2-0.5 [47]	5-10 [39]
Thioridazine	5	0.5-2 [28]	10 [41]
Apocynin	215	10 [29]	> 30 [48] > 300 [39]
Gliotoxin	> 100	3-10 [30]	0.3 [49]

Figure 1

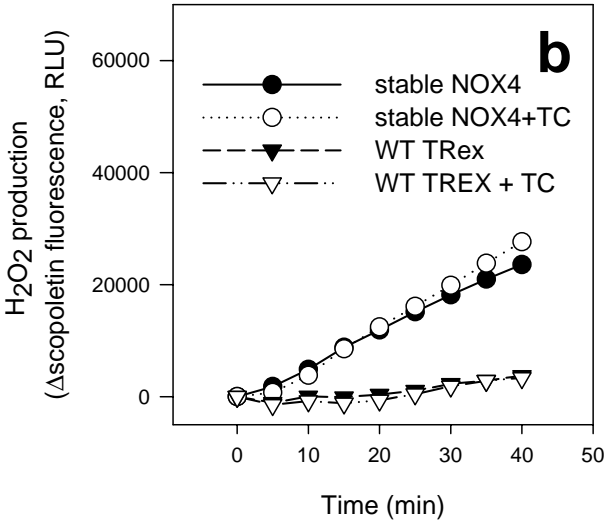
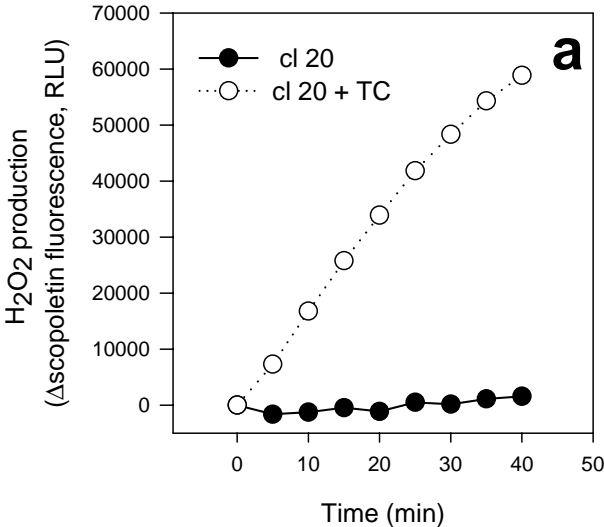


Figure 2

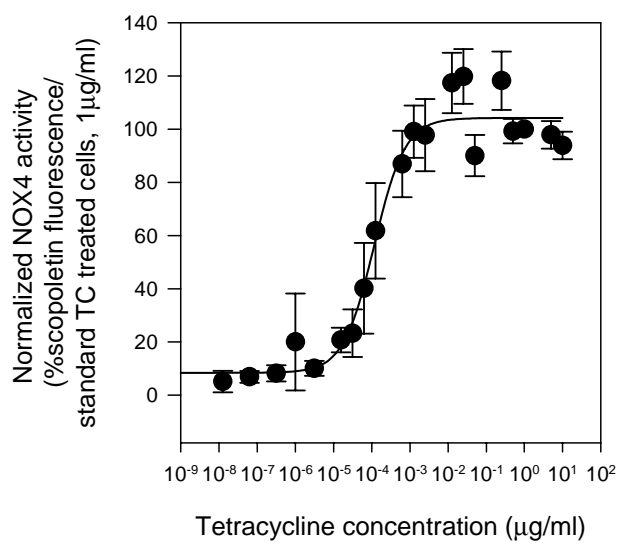


Figure 3

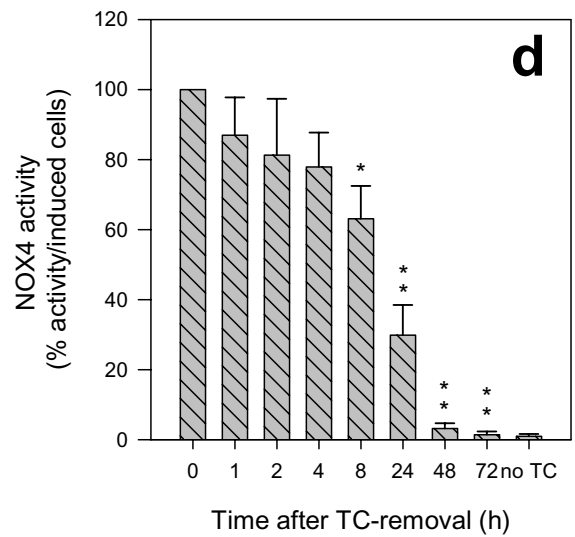
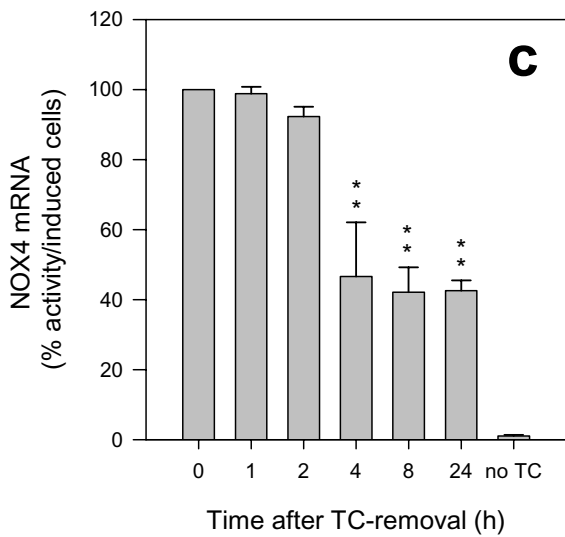
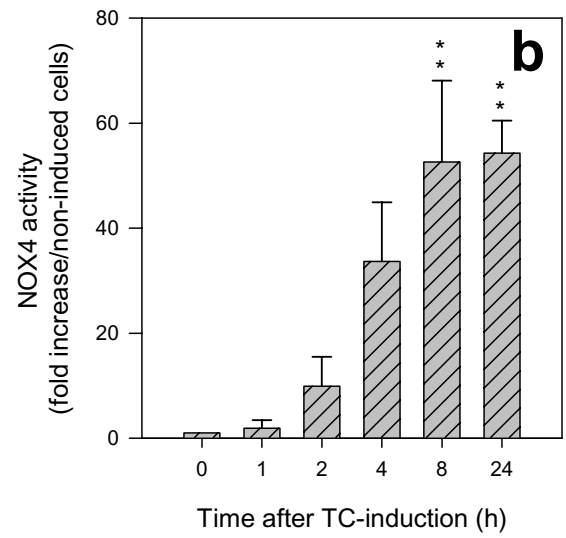
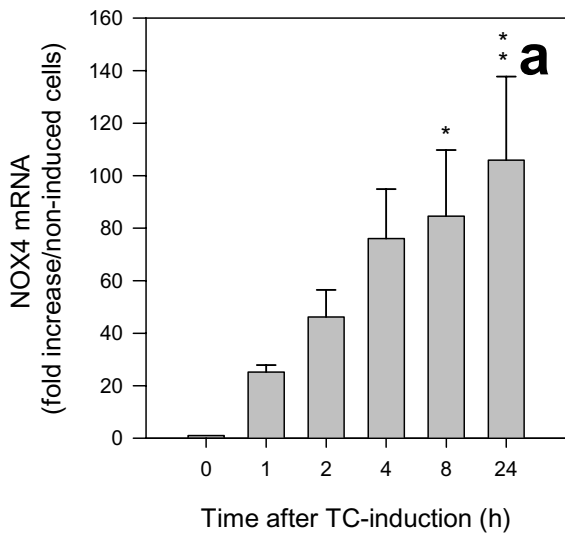


Figure 4

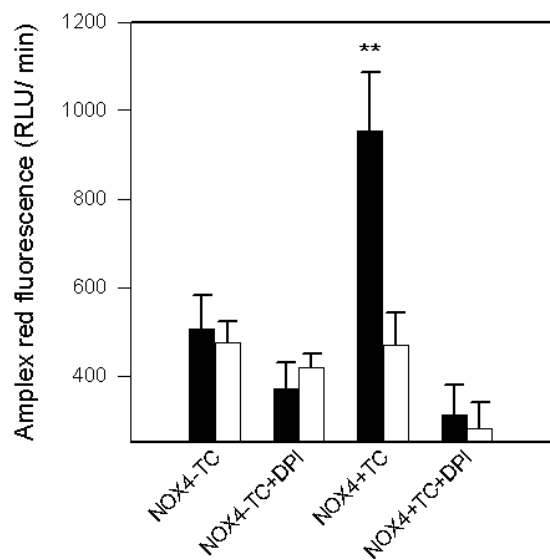


Figure 5

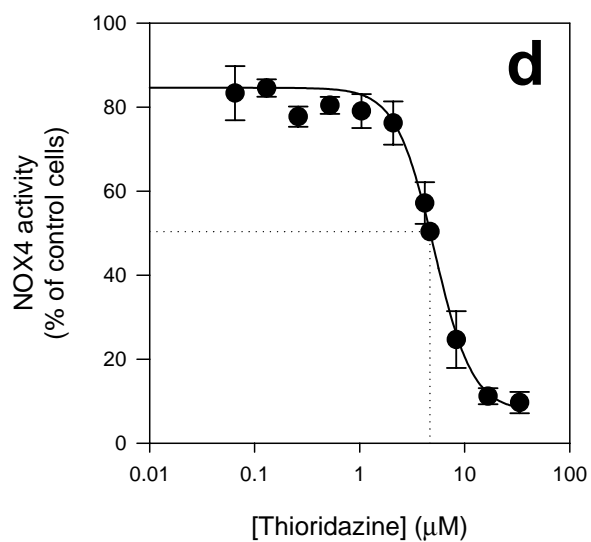
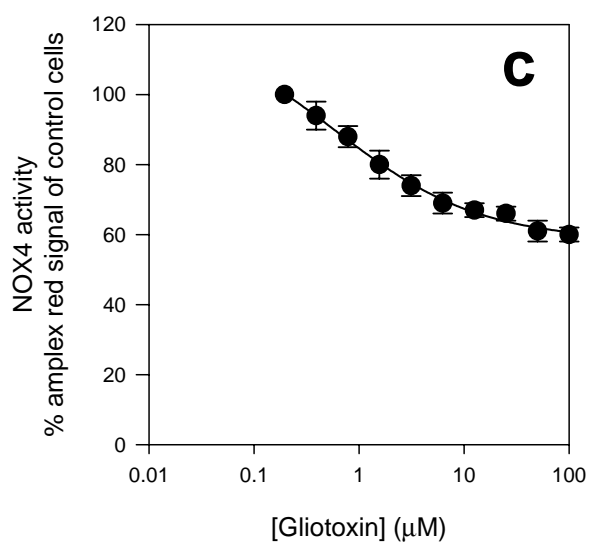
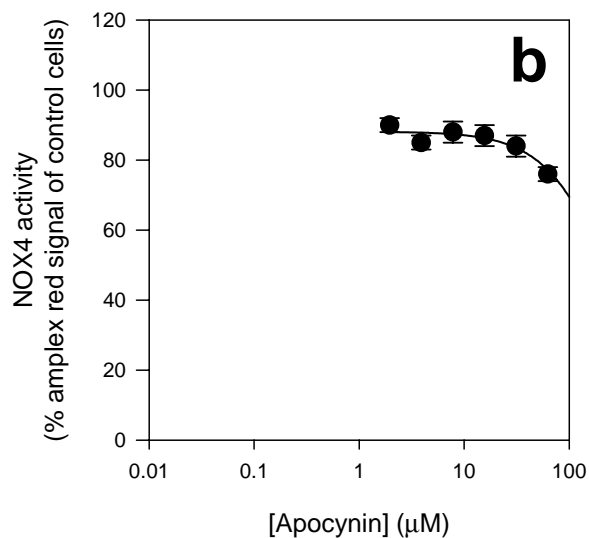
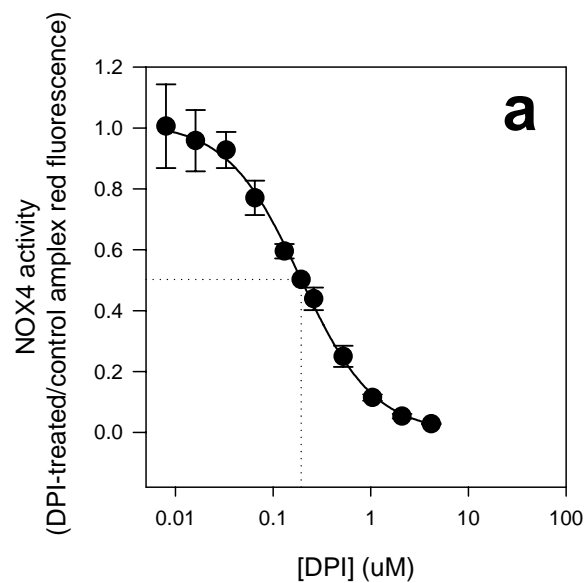


Figure 6

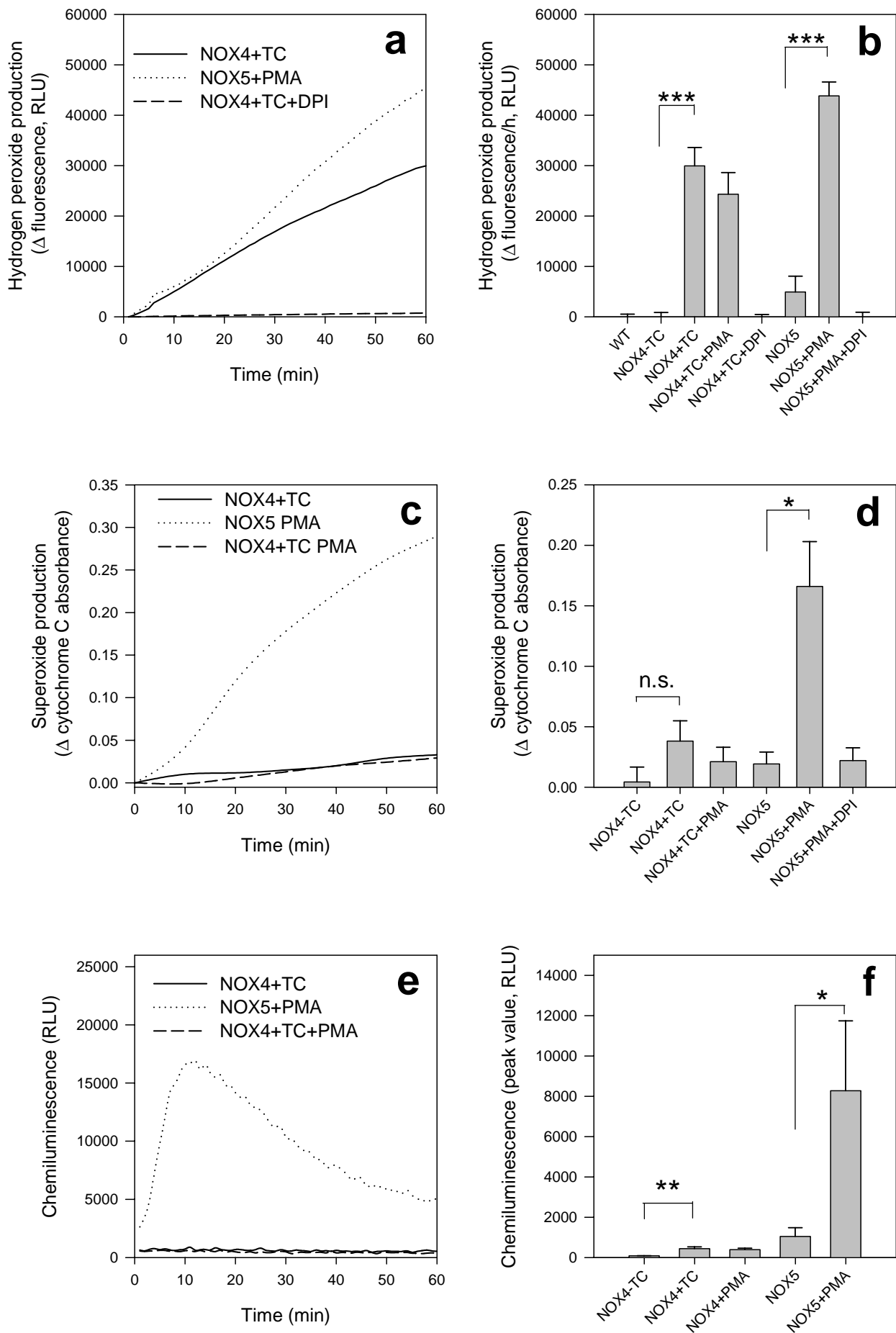


Figure 7

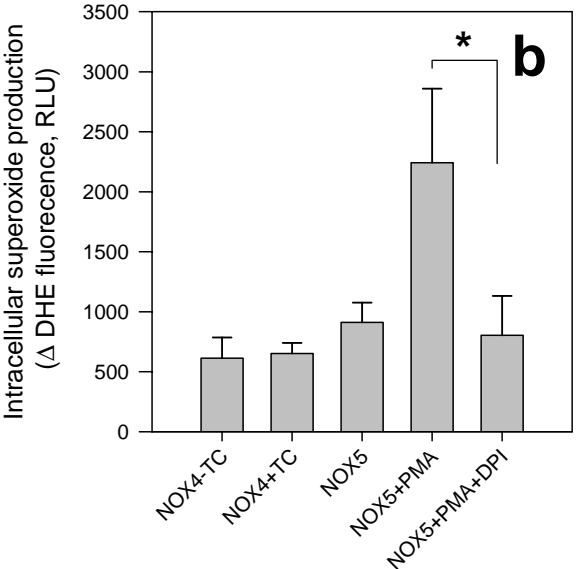
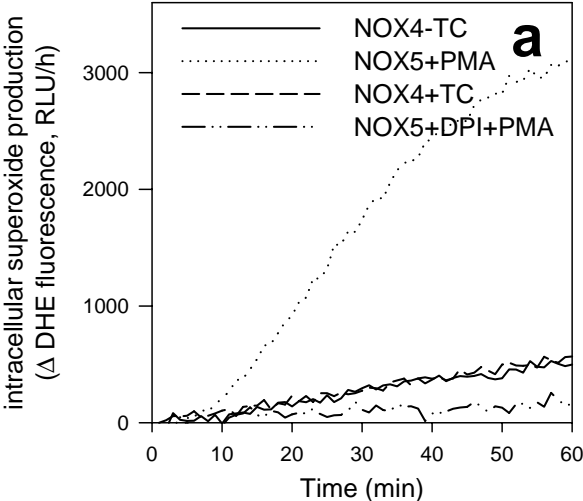




Figure 8

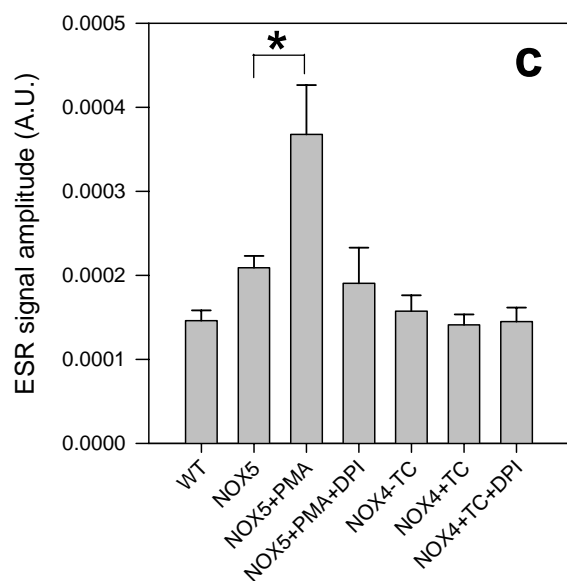
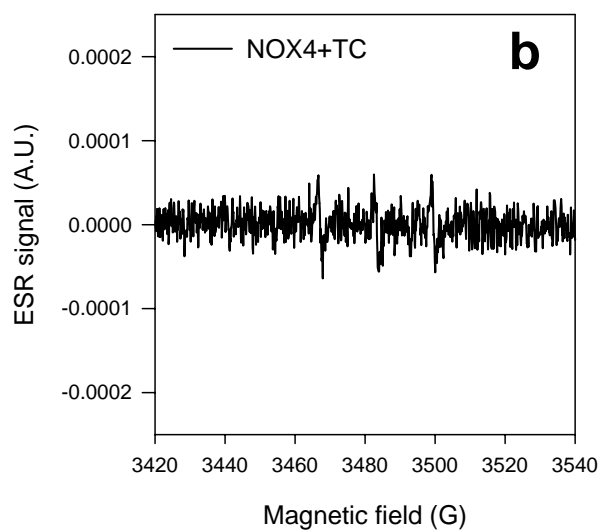
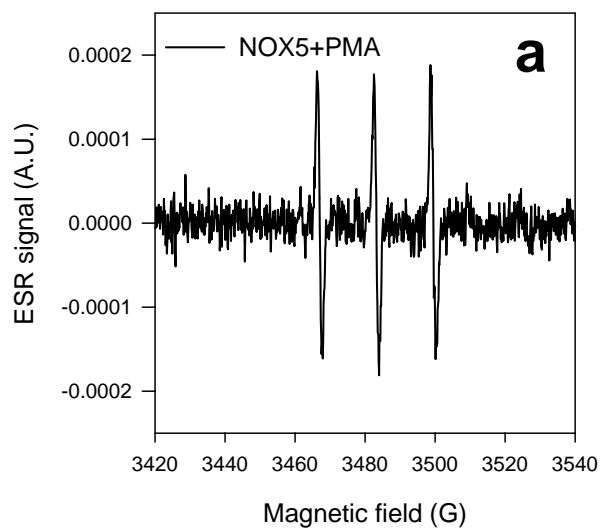


Figure 9

